The Abdus Salam
International Centre for Theoretical Physics

United Nations
Educational, Scientific and
Cultural Organization

IAEA
International Atomic Energy Agency

2045-5

Joint ICTP-INFN-SISSA Conference: Topical Issues in LHC Physics

29 June - 2 July, 2009

Higgs Searches at the Tevatron

Andre SOPCZAK
Lancaster University
UK

Strada Costiera 11, 34014 Trieste, Italy - Tel. +39 040 2240 111; Fax +39 040 224 163 - sci_info@ictp.it, www.ictp.it

What we have learned from Higgs Boson Searches at the Tevatron at the Start of the LHC

André Sopczak
Lancaster University
andre.sopczak@cern.ch

Joint ICTP-INFN-SISSA Conference:
Topical Issues in LHC Physics

1 July 2009

Abstract

Over the last years the Tevatron Run-II has extended several limits on Higgs boson masses and coupling which were pioneered during the LEP accelerator operation between 1989 and 2000. Higgs boson searches will also be at the forefront of research at the LHC. This review concisely discusses the experimental constraints set by the CDF and DØ collaborations in winter 2008/2009 at the beginning of the LHC era. Model-independent and model-dependent limits on Higgs boson masses and couplings have been set and interpretations are discussed both in the Standard Model and in extended models. Recently, for the first time the Tevatron excludes a SM Higgs boson mass range (160-170 GeV) beyond the LEP limit at 95% CL. The experimental sensitivities are estimated for the completion of the Tevatron programme.

Further reading arXiv:0903.4312

Outline

- Introduction
- Production and Decay
- b-Quark Tagging
- Gluon Fusion

gg→H→WW

- Associated

Production

  - WH(H→bb)
  - WH(H→WW)
  - ZH→llbb
  - ZH→ννbb
- H→$\tau\tau$
- H→$\gamma\gamma$
- ttH
- Combined SM Limits
- Beyond the SM
  - bbh, bbH, bbA
  - h,H,A→$\tau\tau$
  - H^+
  - H→$\gamma\gamma$
  - H^{++}
- Conclusions

Introduction

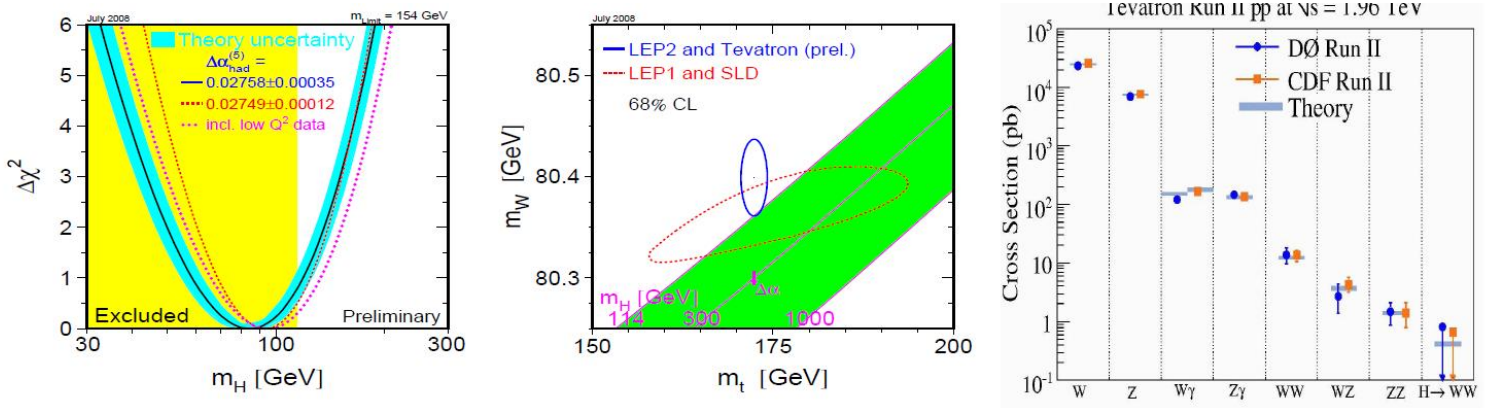

Figure 1. Left: Higgs boson mass prediction in the SM framework. The upper SM Higgs boson mass limit at 95% CL is 154 GeV. Center: smaller ellipse including LEP-2 and Tevatron data (solid line) prefers a region outside the SM Higgs boson mass band ($m_{\mathrm{H}} = 114$ to 1000 GeV). The combined results from LEP-1 and SLD only are shown separately (dashed line). Right: overview of SM measurements by CDF and DØ, and indication of the expected cross-section for a 160 GeV SM Higgs boson.

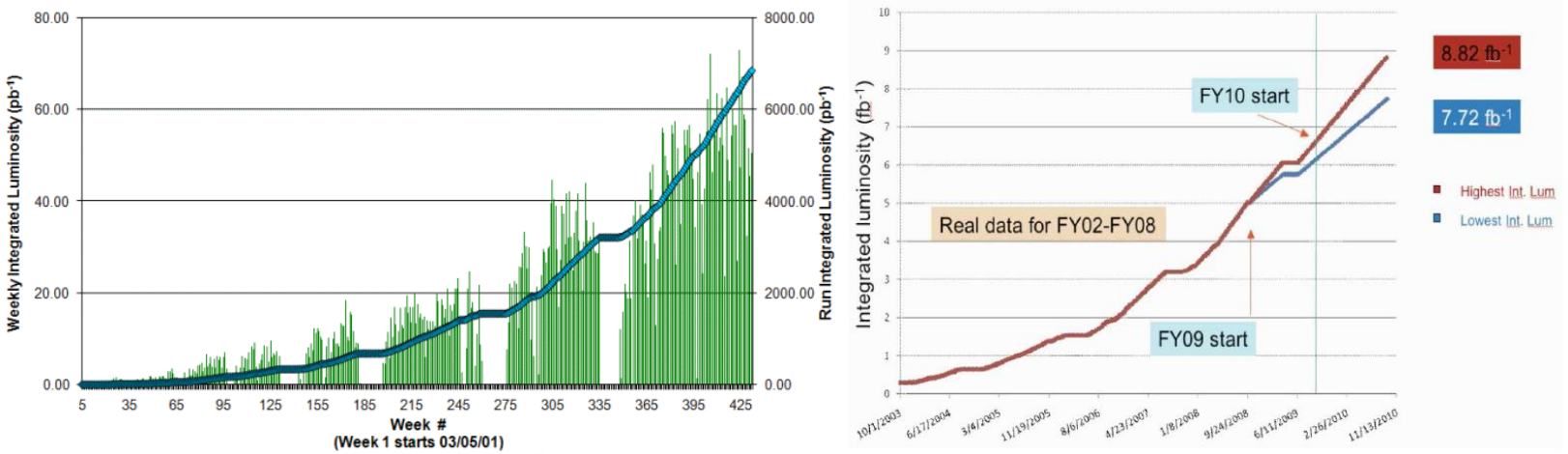

Figure 2. Left: integrated delivered Tevatron luminosity. Right: expectation for 2010 data-taking.

LEP Limits

Table 1. Summary of Higgs boson mass limits at 95% CL. 'LEP' indicates a combination of the results from ALEPH, DELPHI, L3 and OPAL. If results from the experiments are not (yet) combined, examples which represent the different search areas from individual experiments are given. Details are given in Ref. [1].

Search	experiment	limit
Standard Model	LEP	$m_{\mathrm{H}}^{\mathrm{SM}} > 114.4$ GeV
Reduced rate and SM decay		$\xi^2 > 0.05 : m_{\mathrm{H}} > 85$ GeV
		$\xi^2 > 0.3 : m_{\mathrm{H}} > 110$ GeV
Reduced rate and $\mathrm{b\bar{b}}$ decay		$\xi^2 > 0.04 : m_{\mathrm{H}} > 80$ GeV
		$\xi^2 > 0.25 : m_{\mathrm{H}} > 110$ GeV
Reduced rate and $\tau^+\tau^-$ decay		$\xi^2 > 0.2 : m_{\mathrm{H}} > 113$ GeV
Reduced rate and hadronic decay		$\xi^2 = 1 : m_{\mathrm{H}} > 112.9$ GeV
		$\xi^2 > 0.3 : m_{\mathrm{H}} > 97$ GeV
	ALEPH	$\xi^2 > 0.04 : m_{\mathrm{H}} \approx 90$ GeV
Anomalous couplings	L3	$d,\ d_{\mathrm{B}},\ \Delta g_1^{\mathrm{Z}},\ \Delta\kappa_\gamma$ exclusions
MSSM (no scalar top mixing)	LEP	almost entirely excluded
General MSSM scan	DELPHI	$m_{\mathrm{h}} > 87$ GeV, $m_{\mathrm{A}} > 90$ GeV
Larger top-quark mass	LEP	strongly reduced $\tan\beta$ limits
MSSM with CP-violating phases	LEP	strongly reduced mass limits
Visible/invisible Higgs decays	DELPHI	$m_{\mathrm{H}} > 111.8$ GeV
Majoron model (max. mixing)		$m_{\mathrm{H,S}} > 112.1$ GeV
Two-doublet Higgs model	DELPHI	$\mathrm{hA} \to \mathrm{bbbb} : m_{\mathrm{h}} + m_{\mathrm{A}} > 150$ GeV
(for $\sigma_{\max}$)		$\tau^+\tau^-\tau^+\tau^- : m_{\mathrm{h}} + m_{\mathrm{A}} > 160$ GeV
		$(\mathrm{AA})\mathrm{A} \to 6\mathrm{b} : m_{\mathrm{h}} + m_{\mathrm{A}} > 150$ GeV
		$(\mathrm{AA})\mathrm{Z} \to 4\mathrm{b\ Z} : m_{\mathrm{h}} > 90$ GeV
		$\mathrm{hA} \to \mathrm{q\bar{q}q\bar{q}} : m_{\mathrm{h}} + m_{\mathrm{A}} > 110$ GeV
Two-doublet model scan	OPAL	$\tan\beta > 1 : m_{\mathrm{h}} \approx m_{\mathrm{A}} > 85$ GeV
Yukawa process	DELPHI	$C > 40 : m_{\mathrm{h,A}} > 40$ GeV
Singly-charged Higgs bosons	LEP	$m_{\mathrm{H}^\pm} > 78.6$ GeV
$\mathrm{W}^\pm\mathrm{A}$ decay mode	DELPHI	$m_{\mathrm{H}^\pm} > 76.7$ GeV
Doubly-charged Higgs bosons	DELPHI/OPAL	$m_{\mathrm{H}^{++}} > 99$ GeV
$\mathrm{e^+e^-} \to \mathrm{e^+e^-}$	L3	$h_{\mathrm{ee}} > 0.5 : m_{\mathrm{H}^{++}} > 700$ GeV
Fermiophobic $\mathrm{H} \to \mathrm{WW}, \mathrm{ZZ}, \gamma\gamma$	L3	$m_{\mathrm{H}} > 108.3$ GeV
$\mathrm{H} \to \gamma\gamma$	LEP	$m_{\mathrm{H}} > 109.7$ GeV
Uniform and stealthy scenarios	OPAL	depending on model parameters

Production and Decay

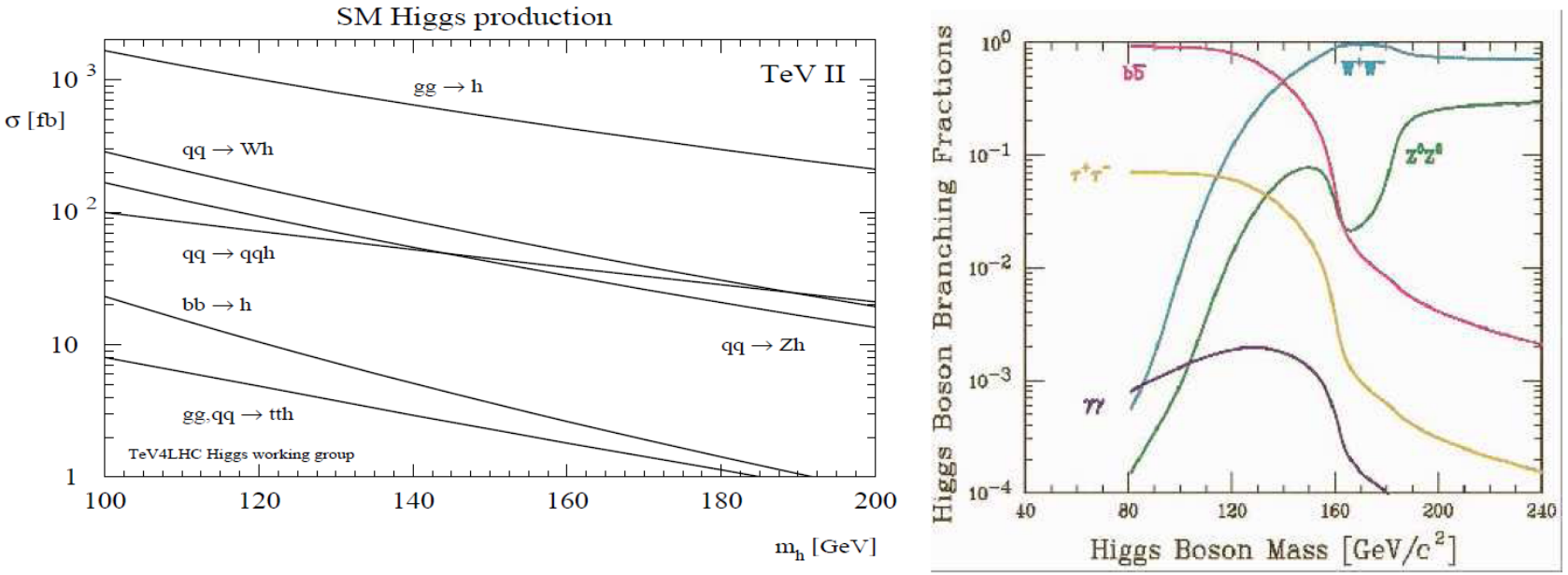

Figure 3. Left: expected SM Higgs boson production cross-sections at the Tevatron (1.96 TeV). Right: expected Higgs boson decay branching ratios for a SM Higgs boson masses. At the Tevatron, $b\bar{b}$ and WW decays are dominant, in addition the $\tau^+\tau^-$ decay mode has a significant contribution.

B-Quark Tagging

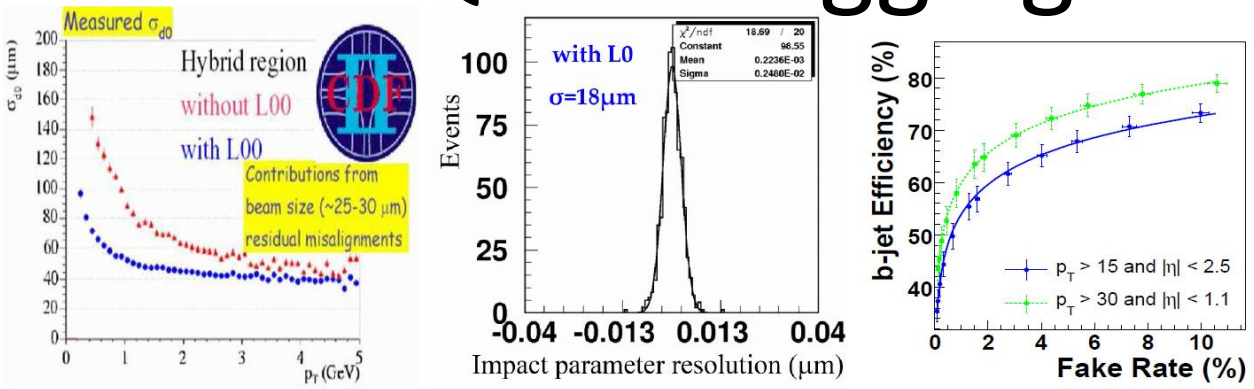

Figure 4. Left: CDF impact parameter resolution as a function of p_T for tracks traversing passive material in vertex detector, with (blue dots) and without (red triangles) use of L00 hits. Center: DØ impact parameter resolution after the installation of a new vertex detector layer (L0), which improved the resolution by 40%. Right: DØ b-quark tagging performance for $Z \rightarrow b\bar{b}$ and $Z \rightarrow q\bar{q}$ events. The error bars include statistical and systematic uncertainties.

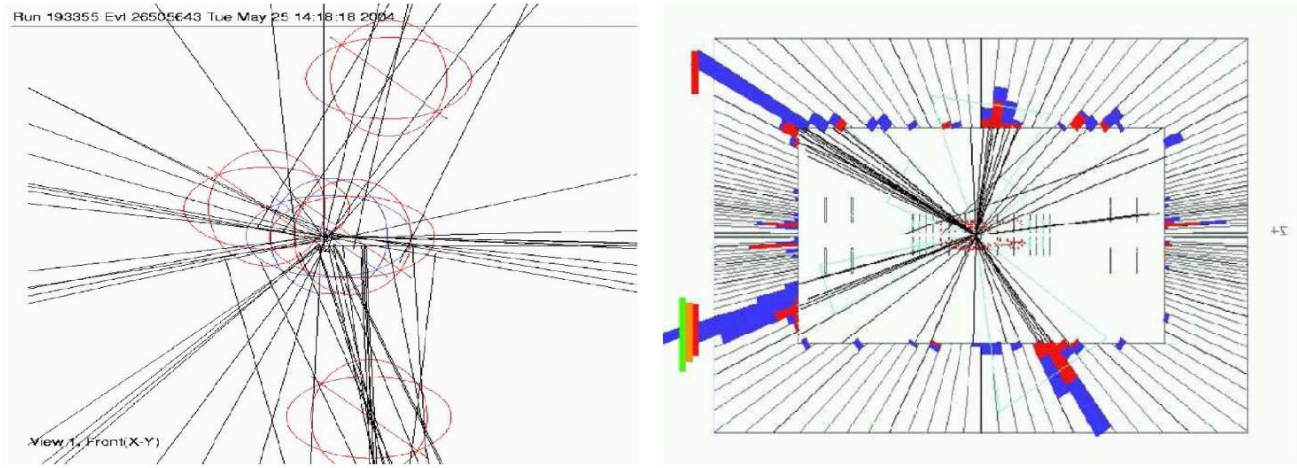

Figure 5. DØ example of b-tagged event. Left: reconstructed tracks near the interaction point. Right: jets clearly visible in the calorimeter.

Z→bb

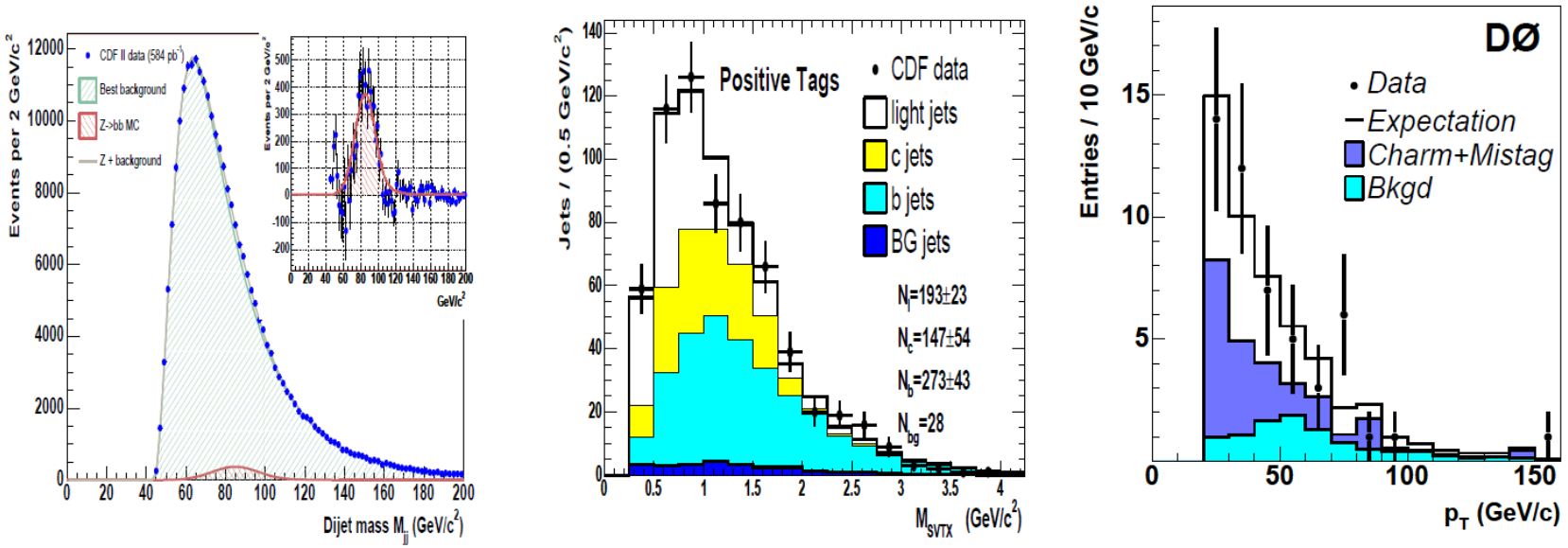

Figure 6. Left: CDF $Z \to b\bar{b}$ signal extracted in double-b-tagged data, relevant for $H \to b\bar{b}$ searches. Center: CDF invariant mass of tracks at the secondary vertex for positively tagged jets. Right: DØ P_t distribution for b-tagged jets of Z + jets events.

Gluon Fusion gg→H→WW

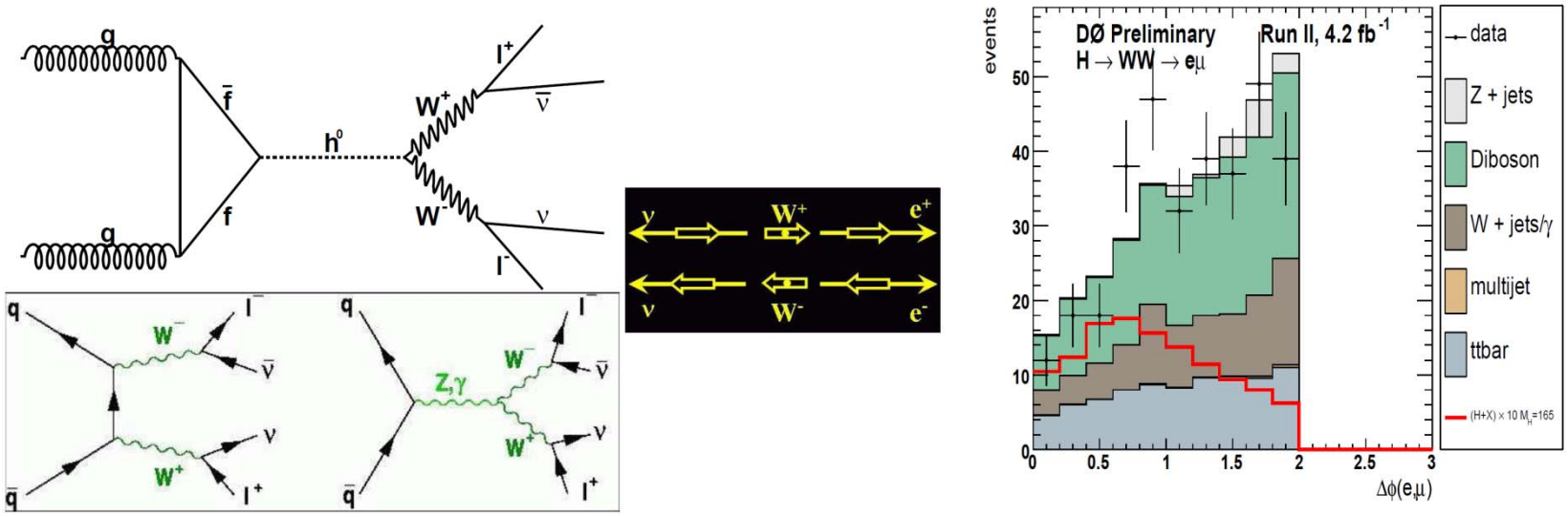

Figure 7. Left: gg → H(H → WW) signal and background processes. Center: indication of spin correlations between final state leptons and W pairs, which lead to different dilepton azimuthal angular ($\Delta\Phi_{ll}$) distributions for signal and background. Right: DØ $\Delta\Phi_{ll}$ distribution for data, and simulated signal and background. $\Delta\Phi_{ll}$ is predicted to be smaller for the signal.

Gluon Fusion gg→H→WW

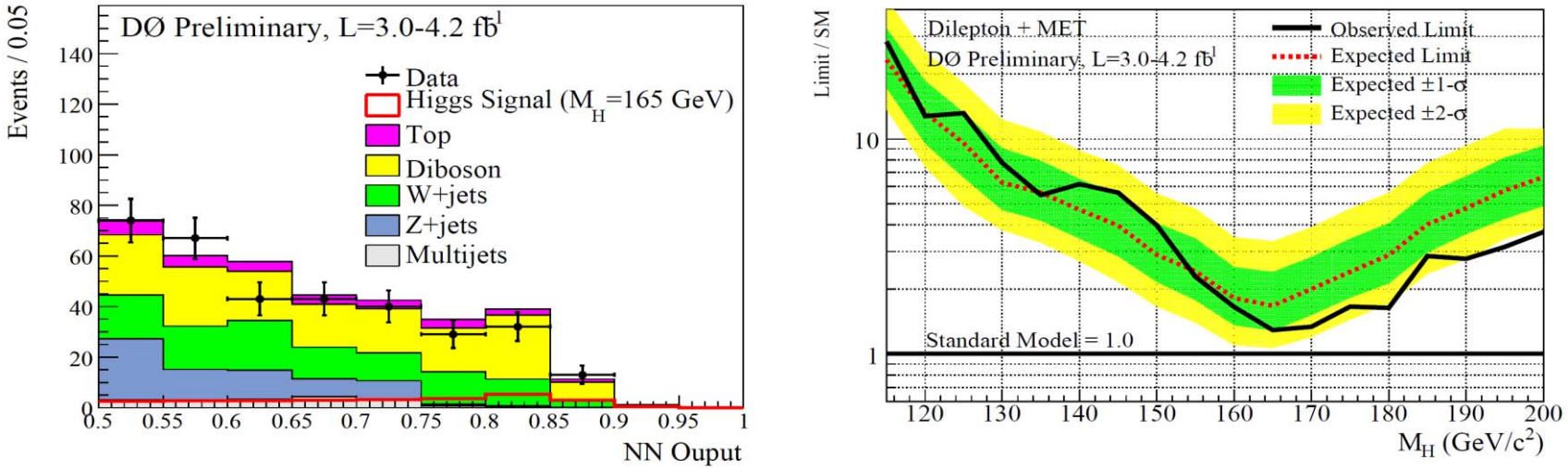

Figure 8. DØ gg → H(H → WW). Left: Neural network output. Right: limit at 95% CL.

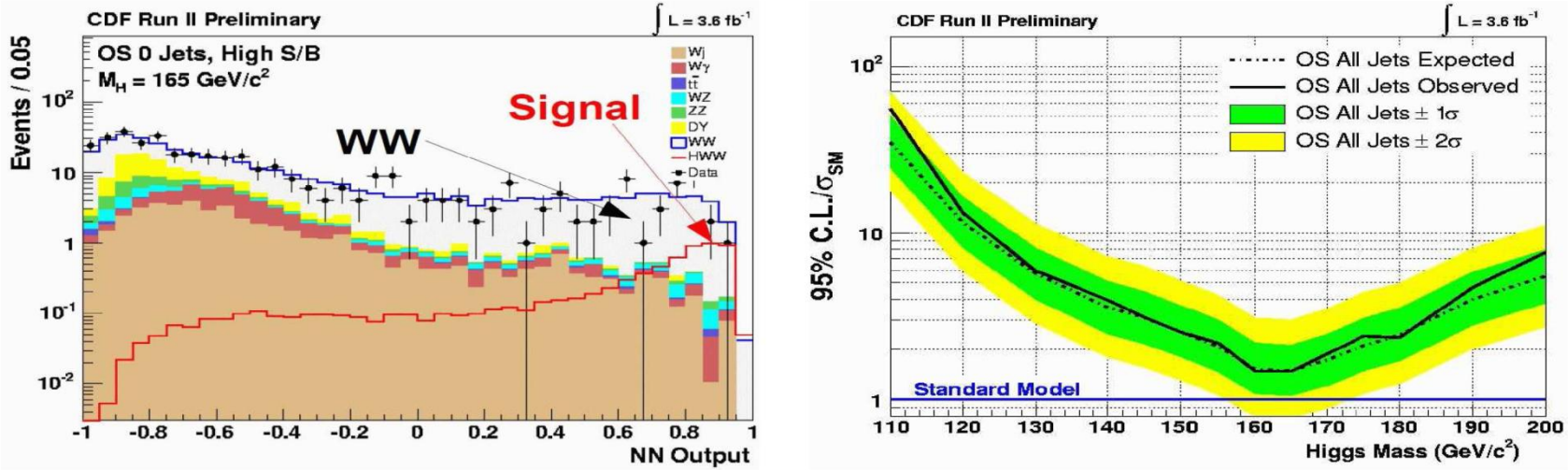

Figure 9. CDF gg → H(H → WW). Left: Neural network output. Right: limit at 95% CL.

Associated Production WH(H→bb)

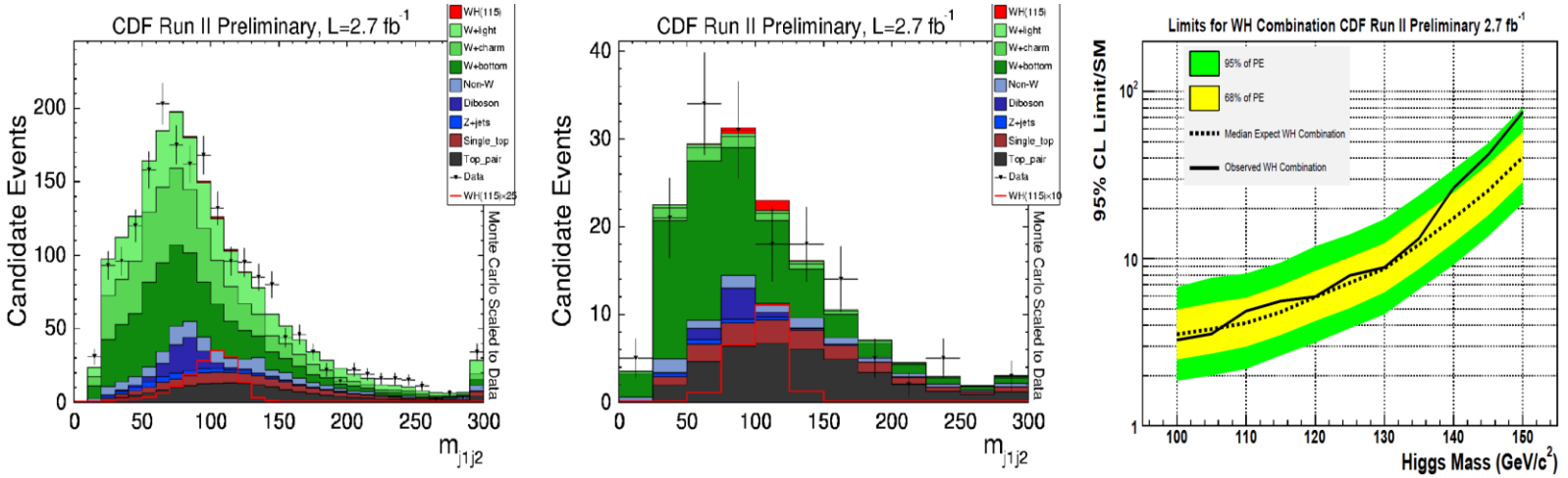

Figure 10. CDF WH($H \rightarrow b\bar{b}$). Matrix Element and Boosted Decision Tree Techniques (ME+BDT). Left: single b-tagging. Center: double b-tagging. Right: limit at 95% CL from combined ME+BDT and neural network analysis results.

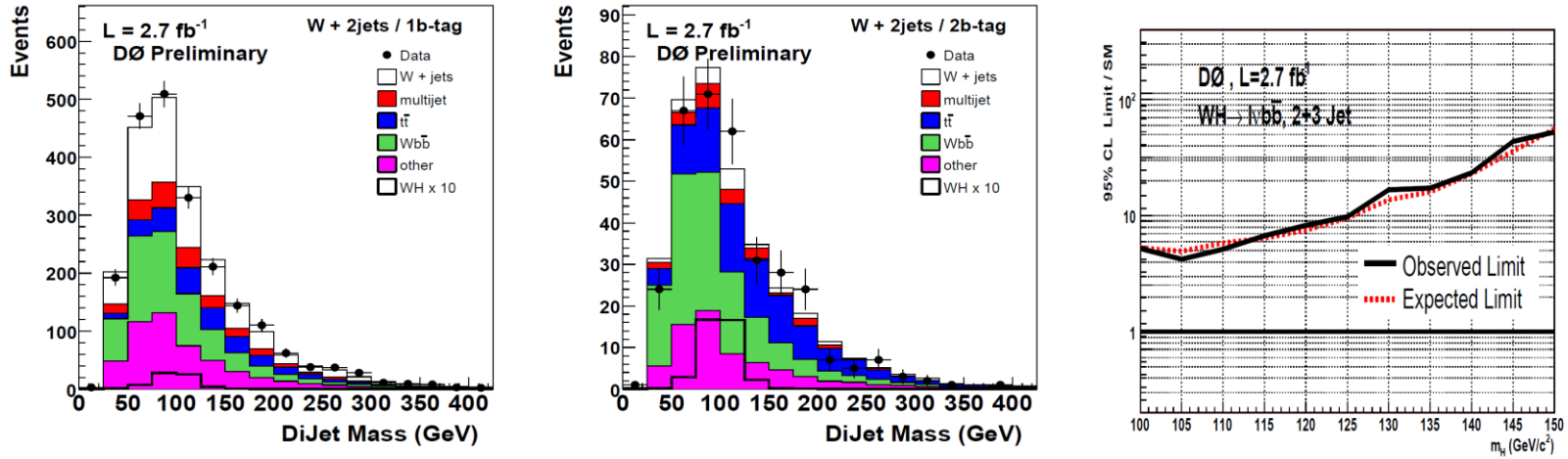

Figure 11. DØ WH($H \rightarrow b\bar{b}$). Left: single b-tagging. Center: double b-tagging. Right: limit at 95% CL.

Associated Production WH(H→WW)

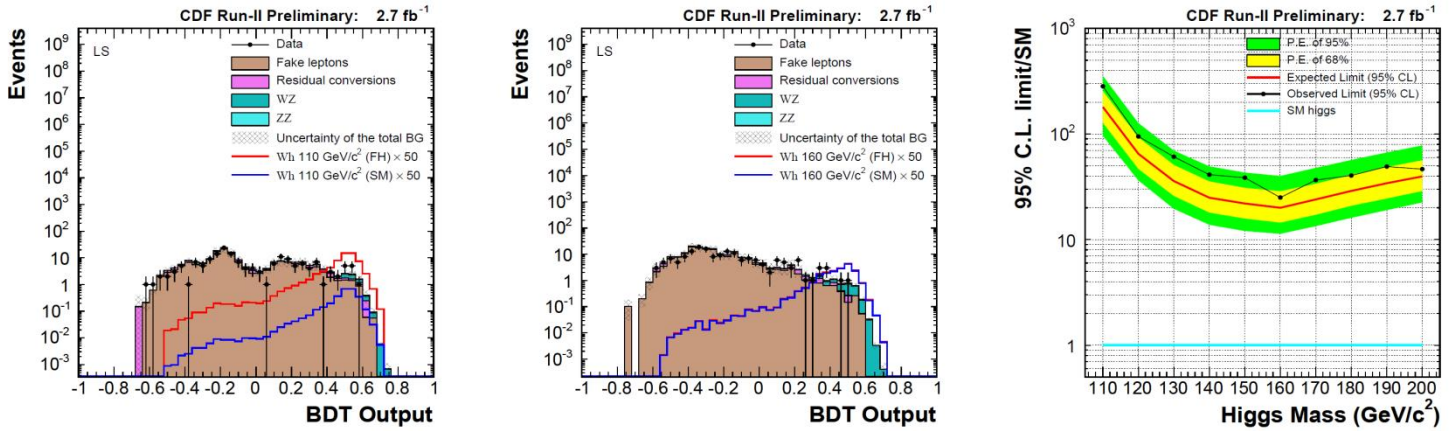

Figure 12. CDF WH(H → WW). Left: comparison of simulated background and observed number of events (110 GeV Higgs boson selection) for the Boosted Decision Tree (BDT) output. Center: comparison of simulated background and observed number of events (160 GeV Higgs boson selection). Right: limit at 95% CL.

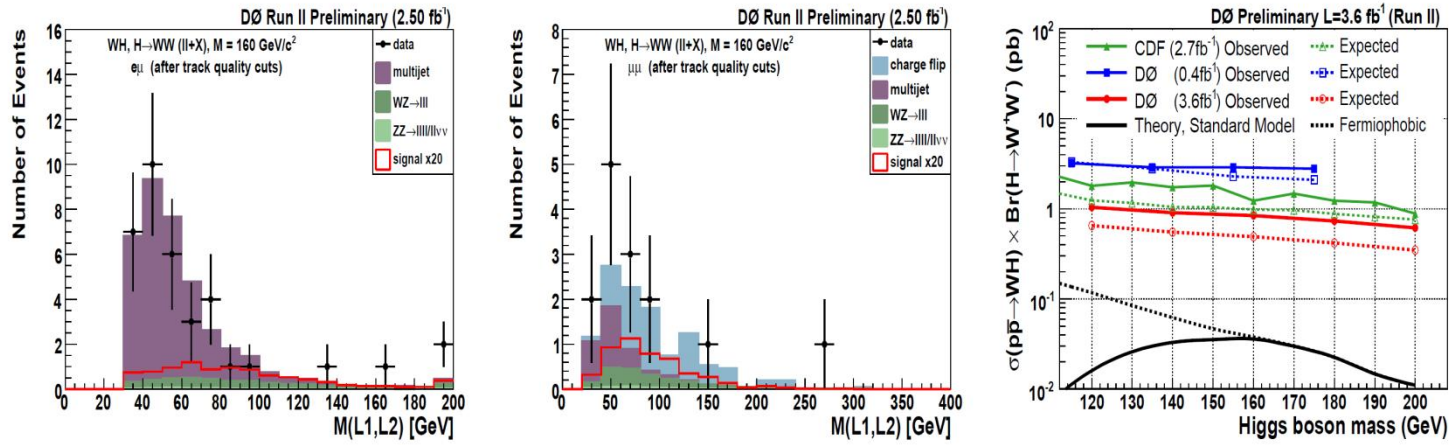

Figure 13. DØ WH(H → WW). Left: eμ invariant mass. Center: $\mu\mu$ invariant mass. Right: limit at 95% CL.

Associated Production ZH→llbb

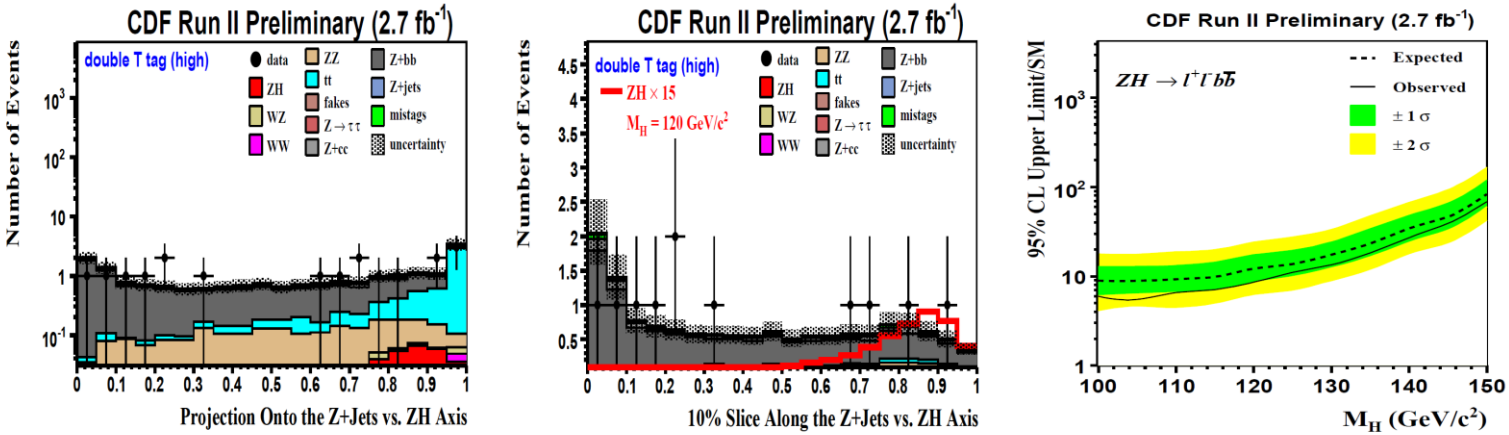

Figure 14. CDF ZH($Z \to \ell\ell$)($H \to b\bar{b}$). Left: $Z \to \ell^+\ell^-$ neural network output (2-dimensional) projection. Mostly Z+jets and $t\bar{t}$ background. Center: $Z \to \ell^+\ell^-$ neural network output (2-dimensional) projection. Right: limit at 95% CL.

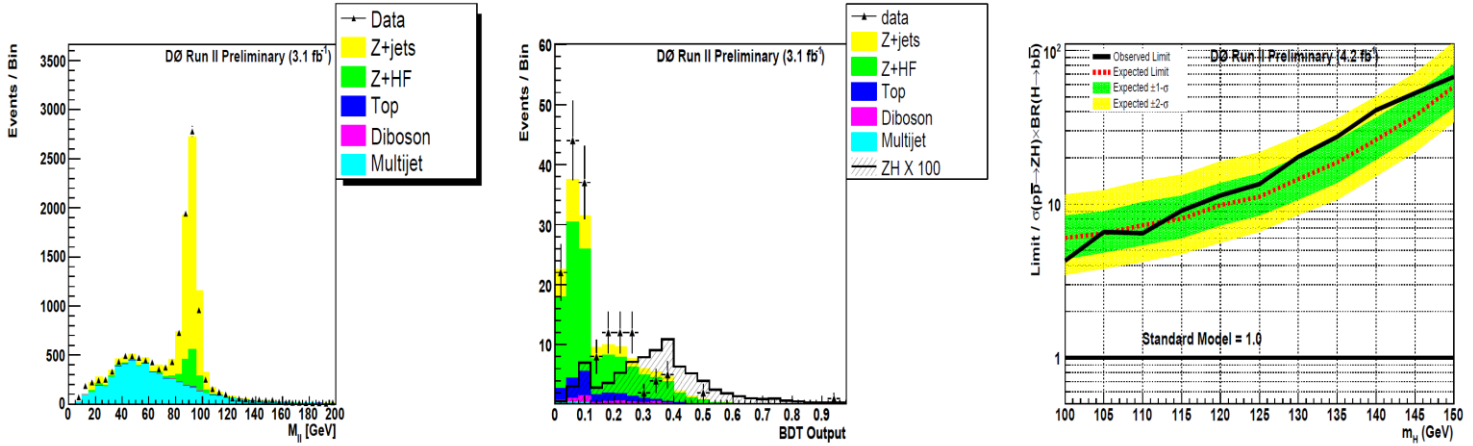

Figure 15. DØ ZH ($Z \to \ell\ell$)($H \to b\bar{b}$). Left: $Z \to e^+e^-$ invariant mass. Center: $Z \to \mu^+\mu^-$ boosted decision tree (BDT) output. Right: cross-section limit combined with previous $Z \to \ell\ell$ results.

Associated Production ZH→ννbb

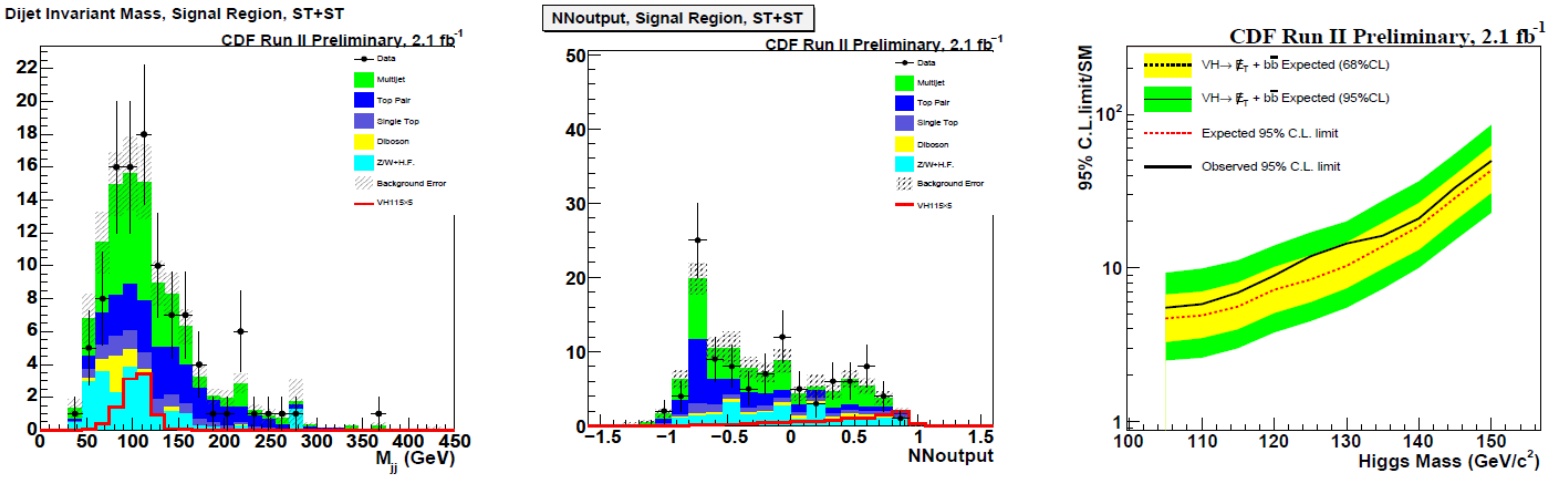

Figure 16. CDF ZH($Z \to \nu\nu$)($H \to b\bar{b}$). Left: invariant di-jet mass. Center: neural network. Right: limit at 95% CL.

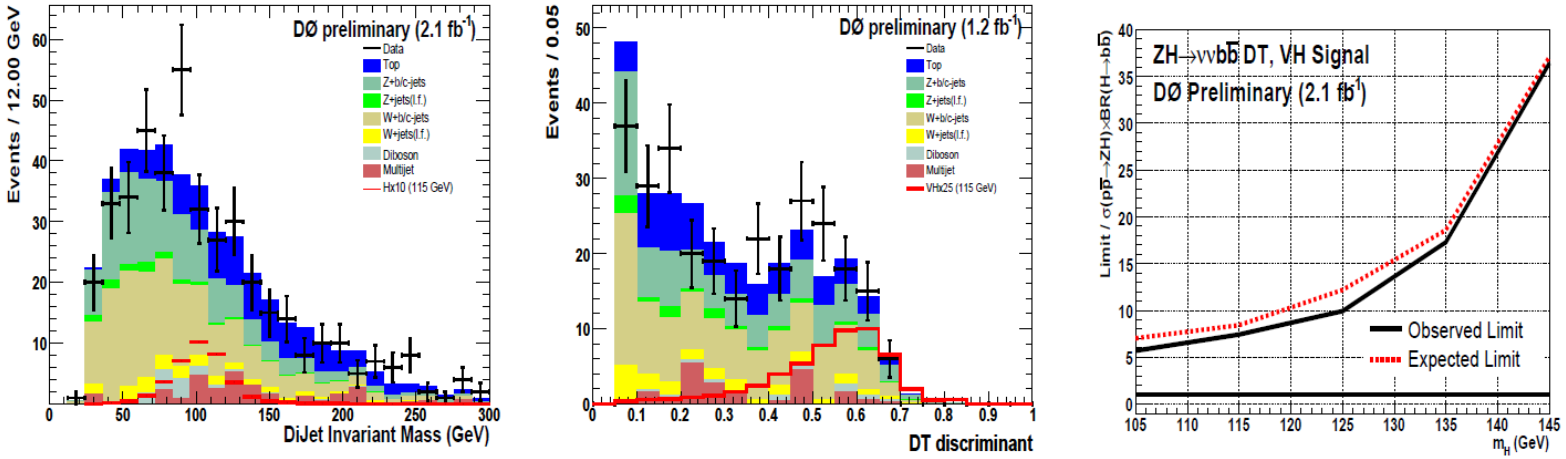

Figure 17. DØ ZH($Z \to \nu\nu$)($H \to b\bar{b}$). Left: invariant di-jet mass. Center: discriminant variable output. Right: limit at 95% CL.

H→ττ

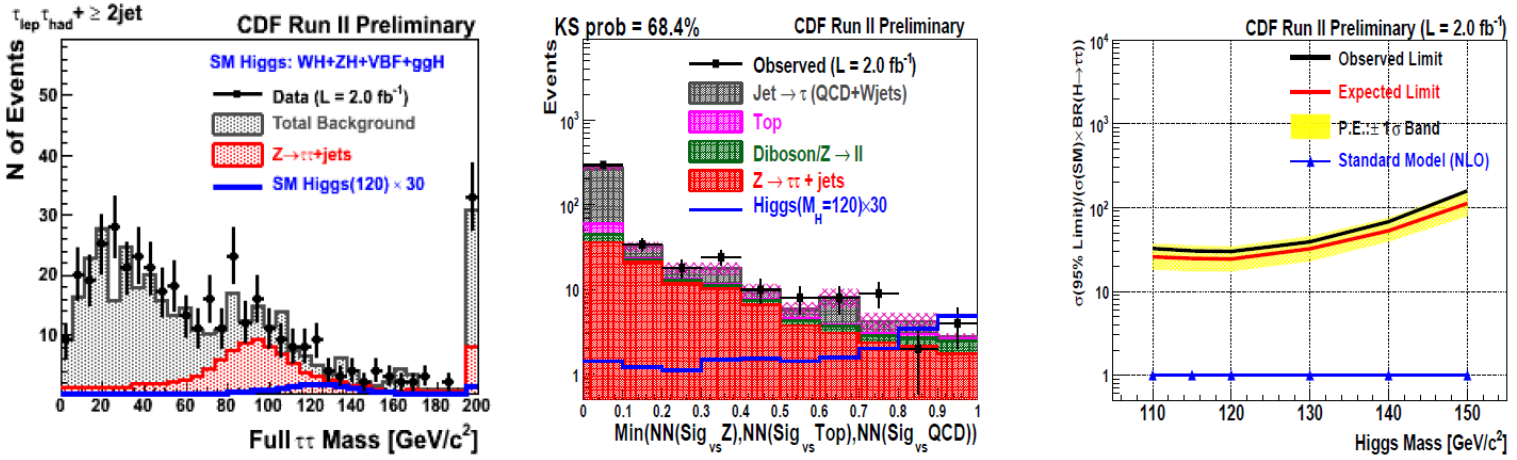

Figure 18. CDF ($H \to \tau^+\tau^-$). Left: invariant mass. Center: neural network output. Right: limit at 95% CL.

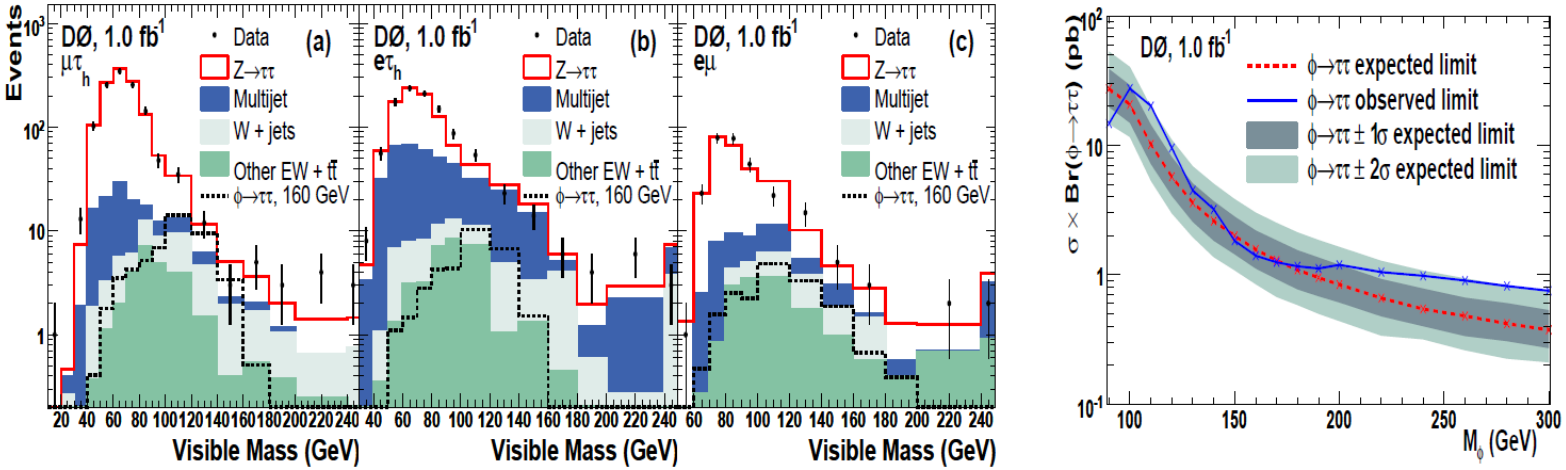

Figure 19. DØ ($H \to \tau^+\tau^-$). Left: invariant masses for $\mu\tau_h$, $e\tau_h$ and $e\mu$. Right: limit at 95% CL.

H→γγ

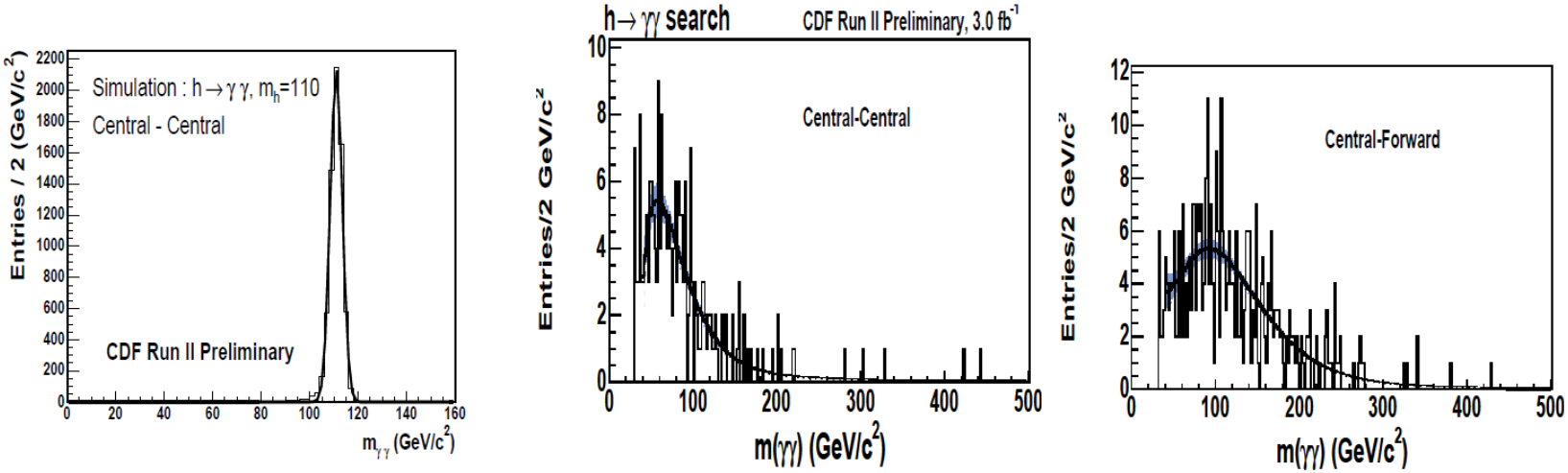

Figure 20. CDF (H → γγ). Left: simulated H → γγ invariant mass. Center: invariant mass spectrum with both photons in the central region. Right: invariant mass spectrum with one photon in the central region and one in the forward region.

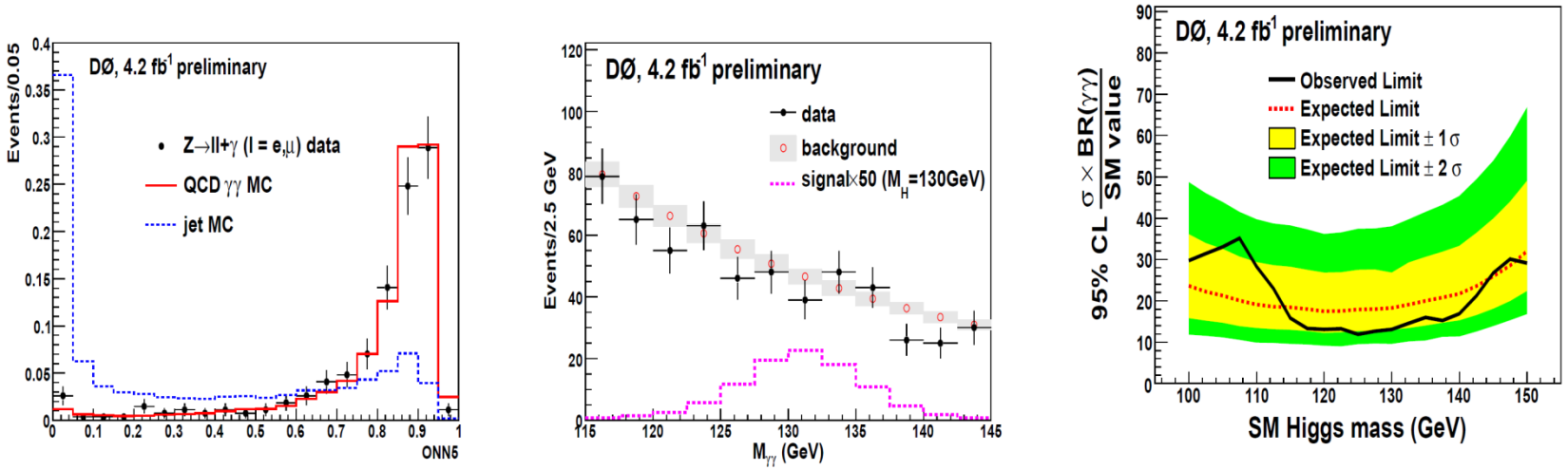

Figure 21. DØ (H → γγ). Left: neural network output. Center: invariant mass. Right: limit at 95% CL.

ttH

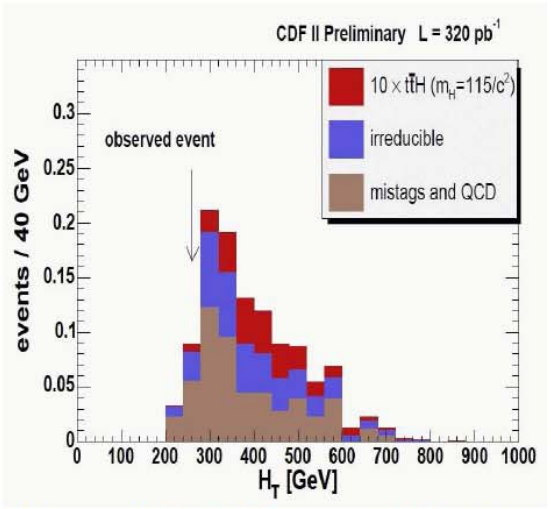

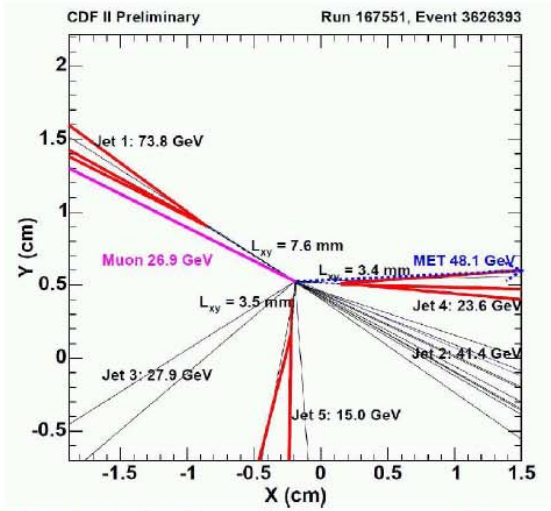

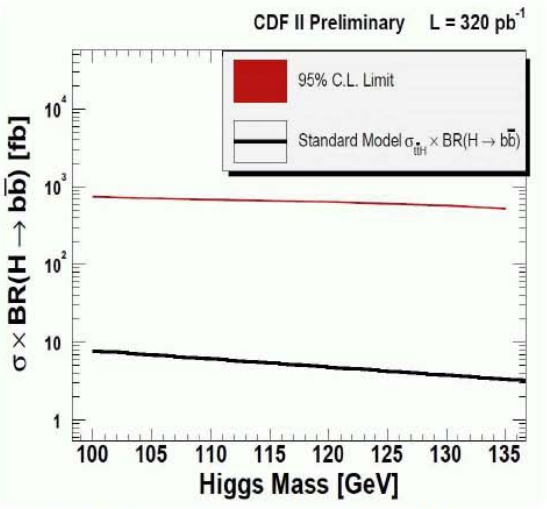

Figure 22. CDF ($t\bar{t} \to t\bar{t}H$). Left: H_T distribution. Center: candidate event. Right: limit at 95% CL.

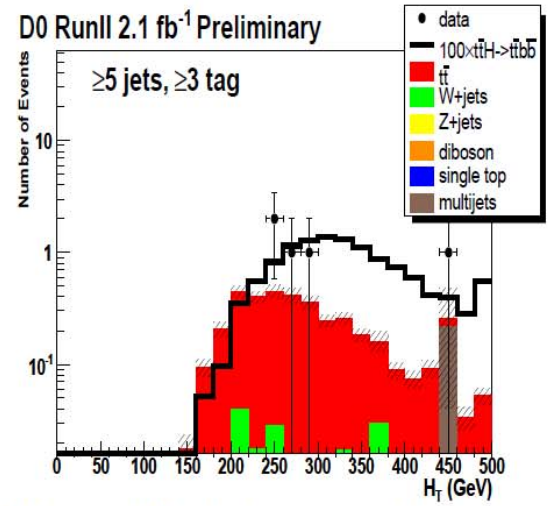

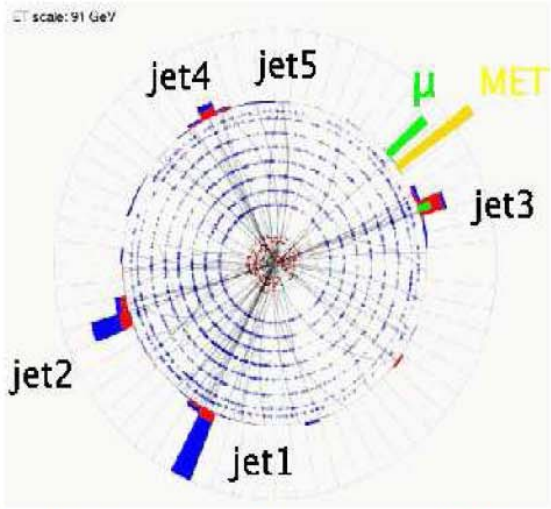

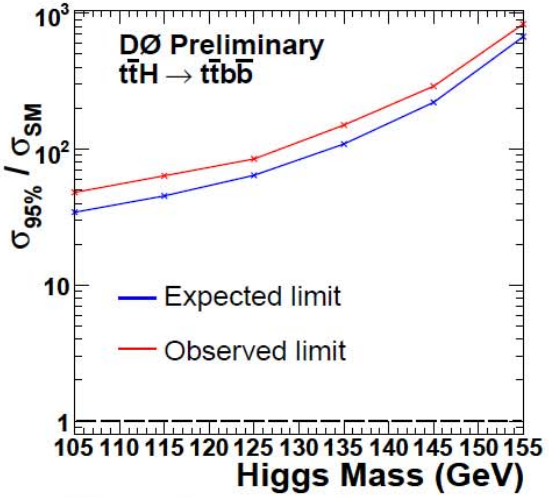

Figure 23. DØ ($t\bar{t} \to t\bar{t}H$). Left: H_T distribution. Center: candidate event. Right: limit at 95% CL.

SM Higgs Boson Summary

Table 2. Summary of observed and expected limits (where available) as factor compated to the SM expectation at 95% CL from CDF and DØ. The note numbers refer to CDF and DØ notes, respectively.

Channel	experiment	m_H (GeV)	$\mathcal{L}$ (fb^{-1})	limit factor obs.	limit factor exp.	Reference note
$H \to WW \to \ell\nu\ell\nu$	CDF	160	3.6	1.5	1.5	9500 [19]
	DØ	160	4.2	1.7	1.8	5871 [18]
$WH \to l\nu b\bar{b}$	CDF	115	2.7	5.6	4.8	9596 [20]
	DØ	115	2.7	6.7	6.4	5828 [21]
$WH \to WWW$	CDF	160	2.7	25	20	7307 [22]
	DØ	160	3.6	10	18	5873 [23]
$ZH \to \ell\ell b\bar{b}$	CDF	115	2.7	7.1	9.9	9665 [24]
	DØ	115	4.2	9.1	8.0	5876 [25]
$ZH \to \nu\bar{\nu}b\bar{b}$	CDF	115	2.1	6.9	5.6	9642 [26]
	DØ	115	2.1	7.5	8.4	5586 [27]
W/ZH, VBF, ggH	CDF	115	2.0	31	25	9248 [28]
$(H \to \tau^+\tau^-)$	DØ	115	1.0	27	28	5883 [29]
$H \to \gamma\gamma$	CDF	–	3.0	–	–	9586 [30]
	DØ	115	4.2	16	19	5858 [31]
$t\bar{t}H$	CDF	–	0.3	–	–	9508 [32]
	DØ	115	2.1	64	45	5739 [33]

Combined SM Higgs Limits and Outlook

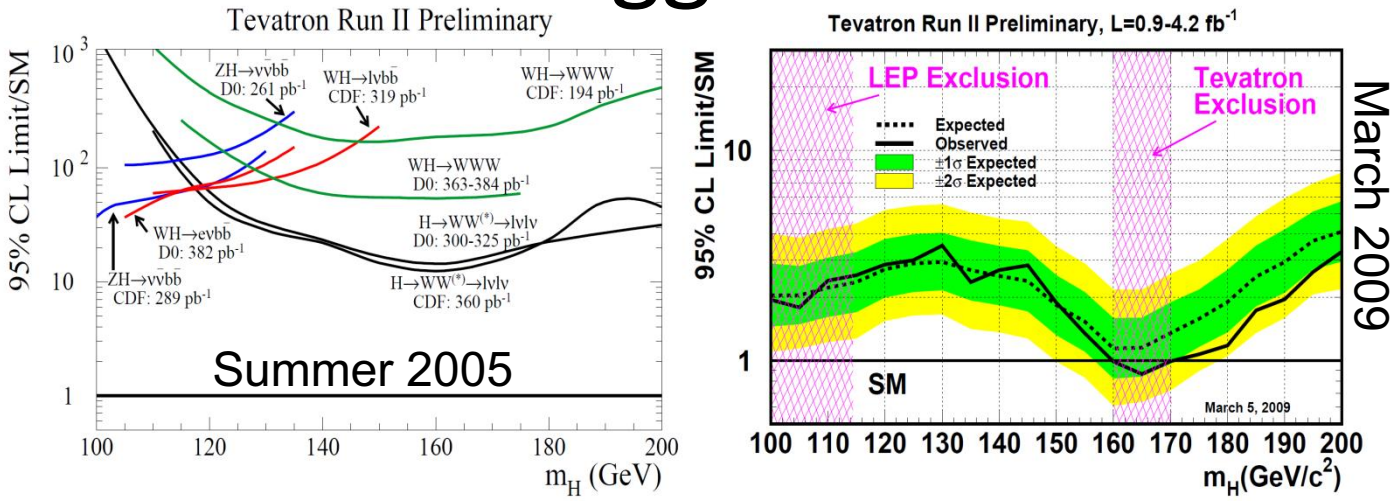

Figure 24. Comparison of progress between summer 2005 and winter 2008/9. Left: ratio of observed cross-section limit and expected SM cross-section, status summer 2005. Right: current combined CDF and DØ limits at 95% CL. Status winter 2008/9: Note that a region between 160 and 170 GeV mass is excluded.

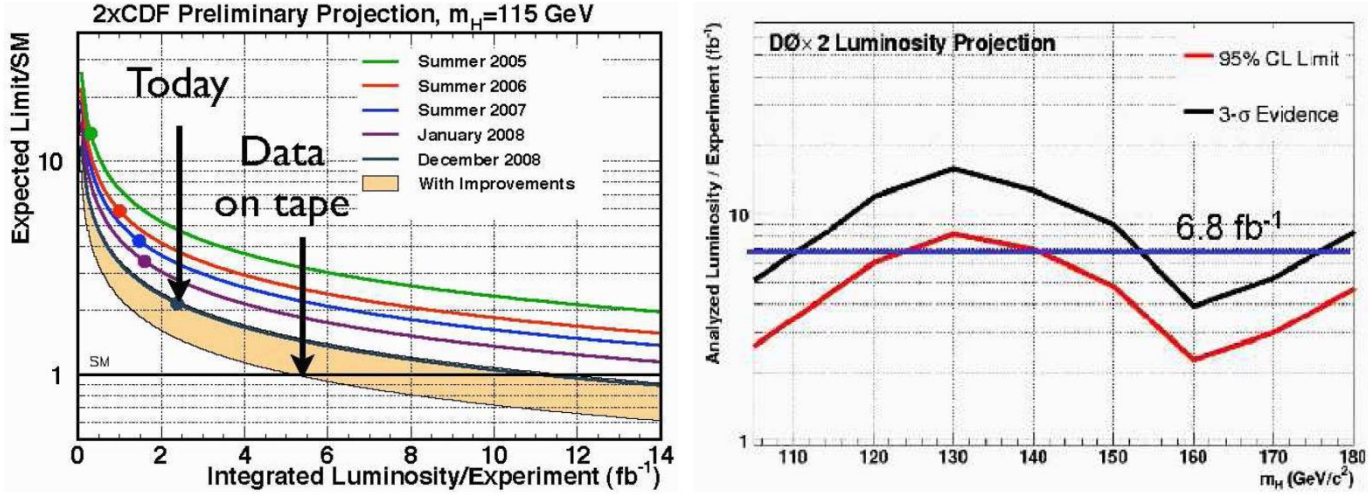

Figure 25. Outlook. Left: for a 115 GeV Higgs boson. Right: for a mass range between 105 to 180 GeV.

Beyond the SM: bbh, bbH, bbA

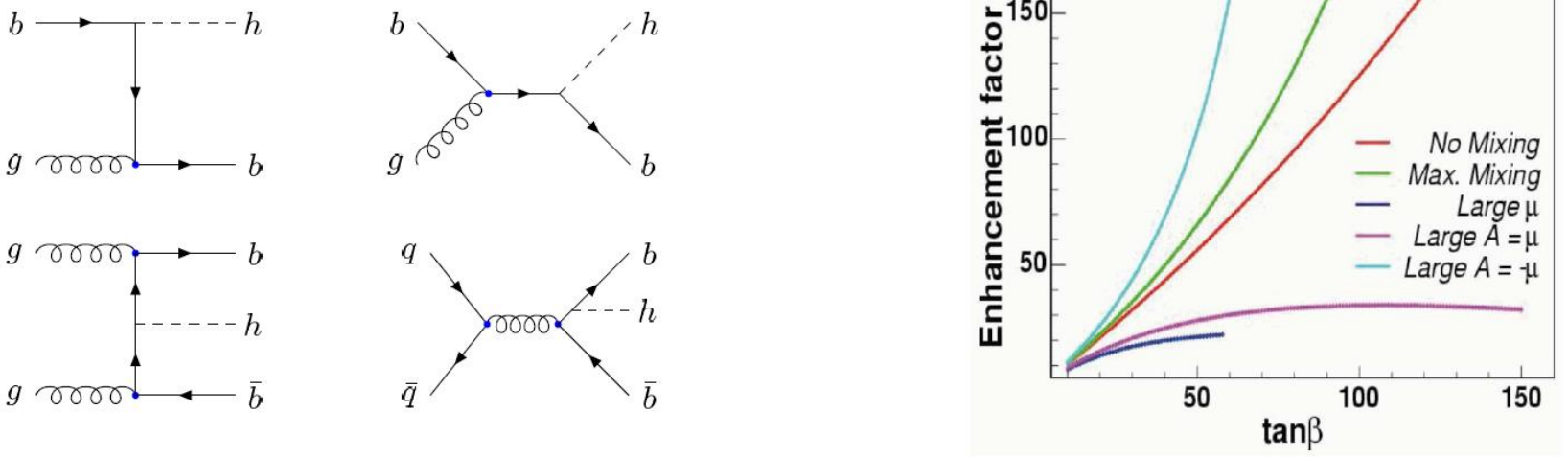

Figure 26. DØ. Left: leading-order Feynman diagrams for neutral Higgs boson production in the five-flavor scheme (top) and four-flavor scheme (bottom). Right: enhancement factor as a function of tan β.

Beyond the SM: bbh, bbH, bbA

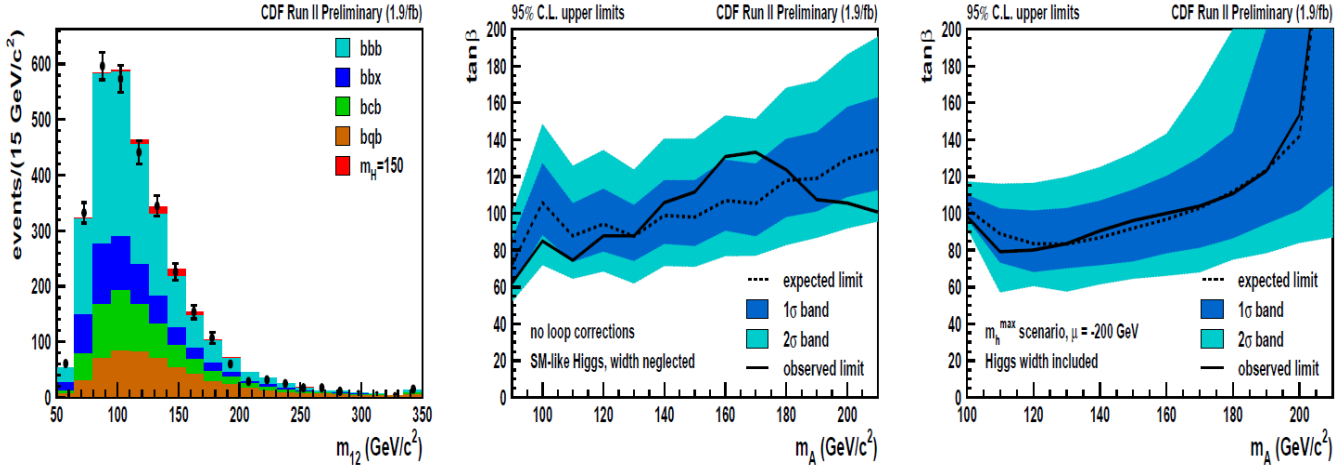

Figure 27. CDF. $b\bar{b}A(A \to b\bar{b})$. Left: invariant mass of the two most energetic jets $m_A = 150$ GeV. Center: limits on $\tan\beta$ in the gereral Two Higgs Doublet Model (THDM). Right: limits on $\tan\beta$ in the MSSM for the mhmax scenario.

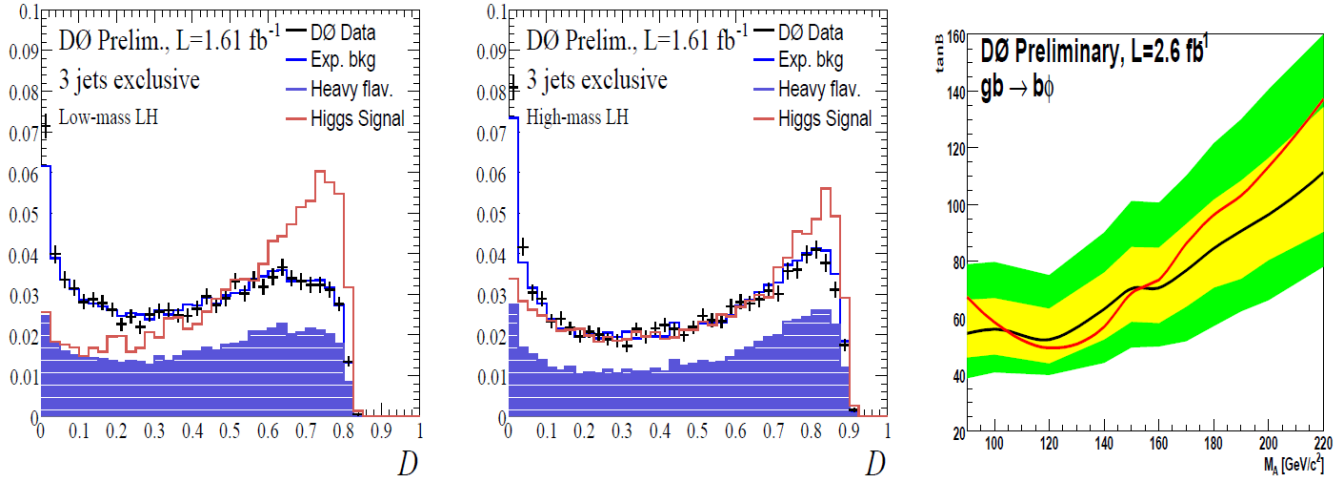

Figure 28. DØ. $b\bar{b}A(A \to b\bar{b})$. Left: discriminant variable output, low-mass. Center: discriminant variable output, high-mass. Right: limit at 95% CL.

Beyond the SM: h,H,A→ττ

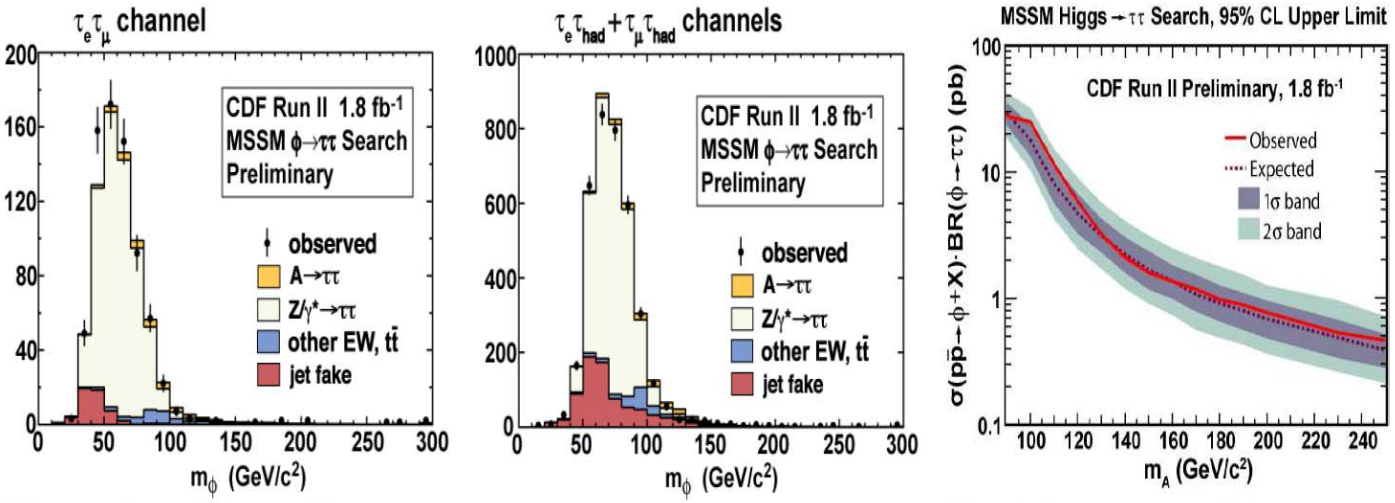

Figure 29. CDF. Left: invariant mass eμ channel for $\Phi = A$ with $m_A = 140$ GeV. Center: invariant mass $\ell\tau_h$ channel where ℓ represents an electron or a muon. Right: cross-section limit at 95% CL.

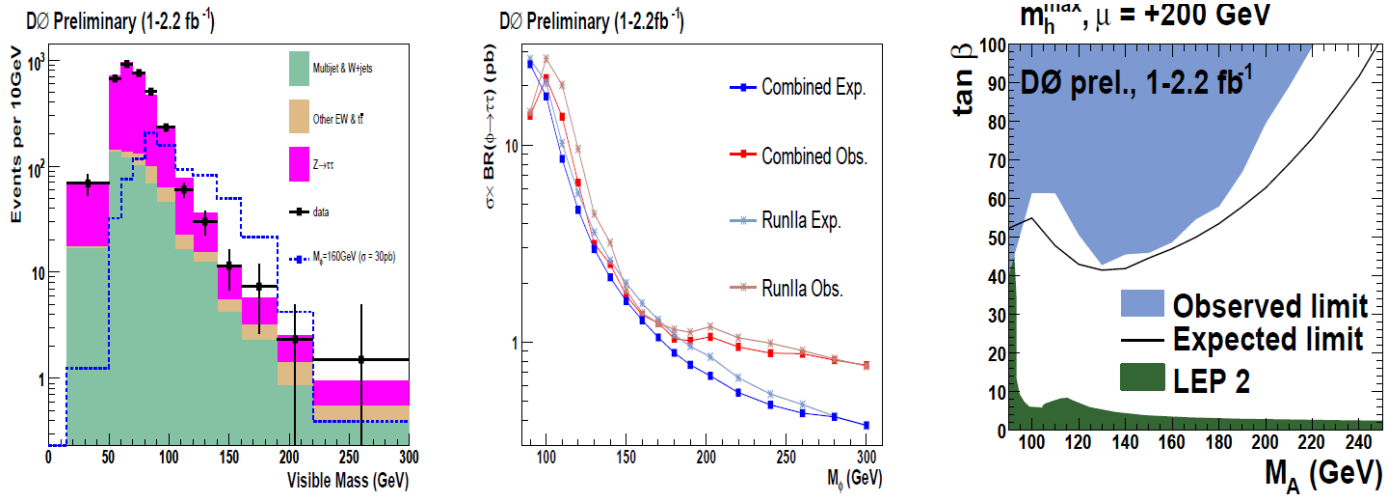

Figure 30. DØ. Left: visible mass for $\Phi = A$ with $m_A = 160$ GeV. Center: cross-section limit at 95% CL. Right: MSSM limit at 95% CL.

Beyond the SM: H^+ ($\rightarrow \tau\nu$,cs)

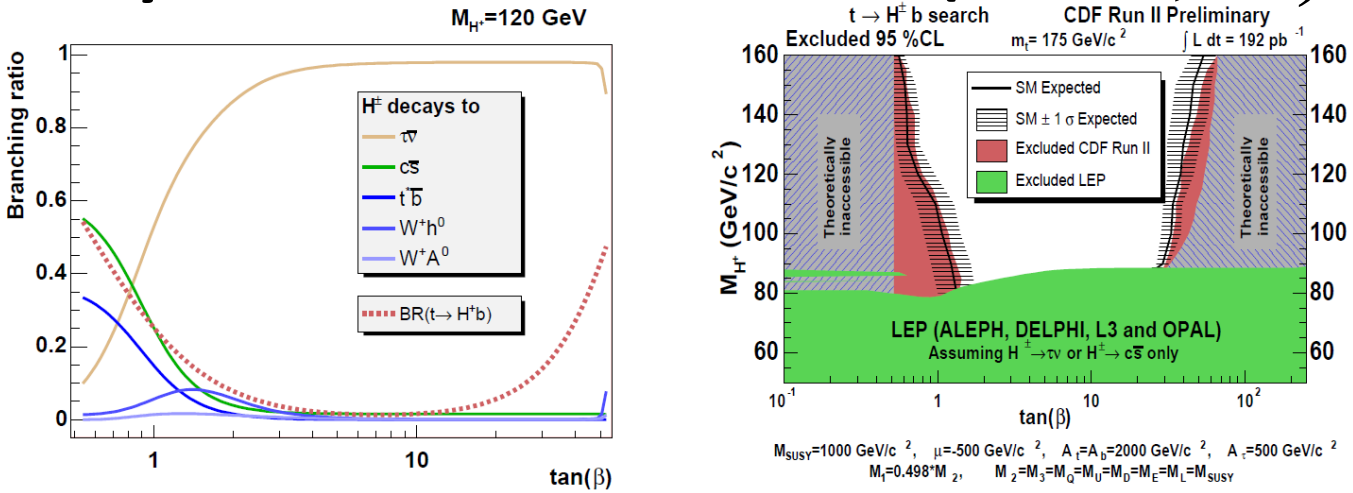

Figure 31. Left: branching ratios for a 120 GeV charged Higgs boson production in top decays and charged Higgs boson decays as a function of tan β in the MSSM. Right: CDF. Limits on the charged Higgs boson mass as function of tan β for a specific set of MSSM parameters.

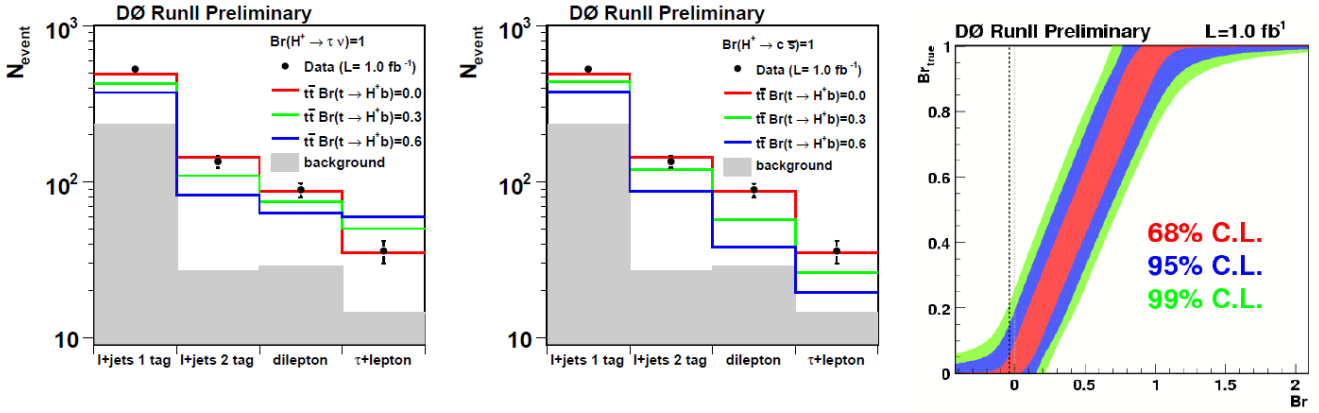

Figure 32. DØ. Left: variation of number of expected events for $t \rightarrow H^+b$ ($H^+ \rightarrow \tau^+\nu$). Center: variation of number of expected events for $t \rightarrow H^+b$ ($H^+ \rightarrow cs$). Right: BR($t \rightarrow H^+b$) limits and type II THDM leading order calculation expectation.

Beyond the SM: H^+ ($\rightarrow \tau\nu$,cs)

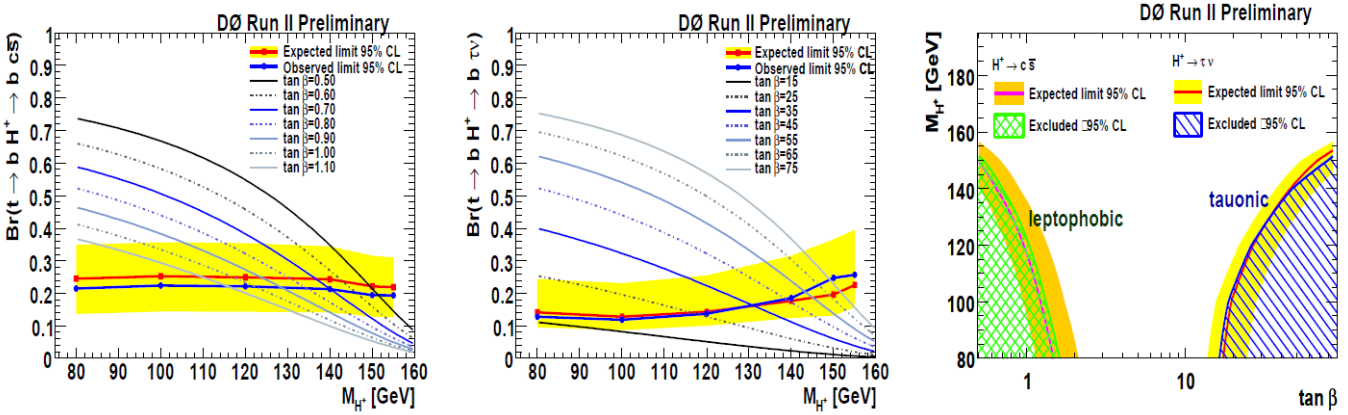

Figure 33. DØ. Left: BR(t $\rightarrow$ H$^+$b)($H^+ \rightarrow cs$) limit at 95% CL. Center: BR(t $\rightarrow$ H$^+$b)($H^+ \rightarrow \tau^+\nu$) limit at 95% CL. Right: limits on the charged Higgs boson mass as function of tan β for a specific set of MSSM parameters.

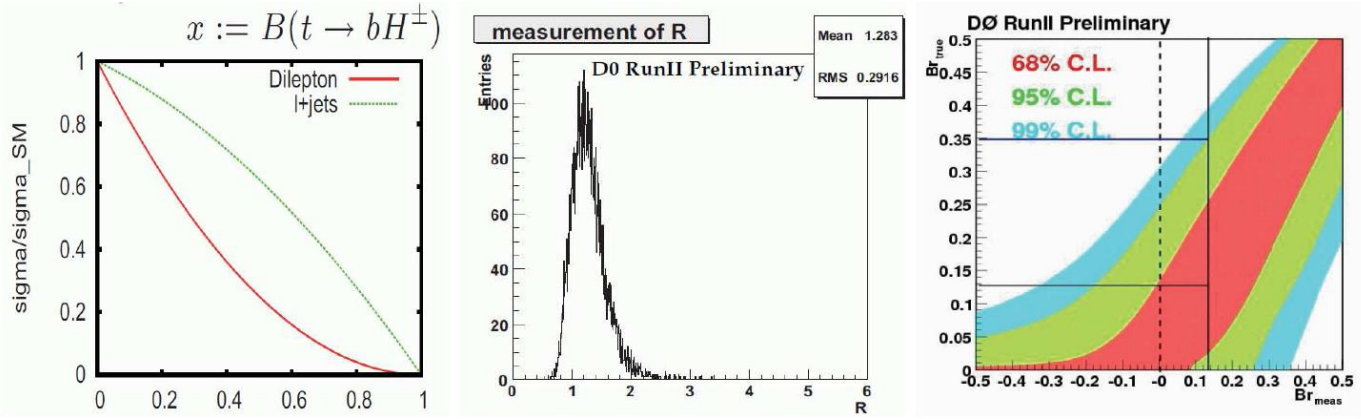

Figure 34. DØ. Left: modified cross-sections relative to the SM cross-section as functions of BR(t $\rightarrow$ H$^+$b). Center: cross-section ratio, R, distribution generated from the 10,000 pseudo-experiments. Right: Feldman-Cousins confidence interval bands as functions of measured and generated branching fraction BR(t $\rightarrow$ H$^+$b). For a leptophobic 80 GeV charged Higgs boson, BR($H^+ \rightarrow$ cs)=1, BR(t $\rightarrow$ H$^+$b) limits at 95% CL are 0.35 (observed, solid line) and 0.25 (expected, dotted line).

Beyond the SM: H^+ (→cs) and (→tb)

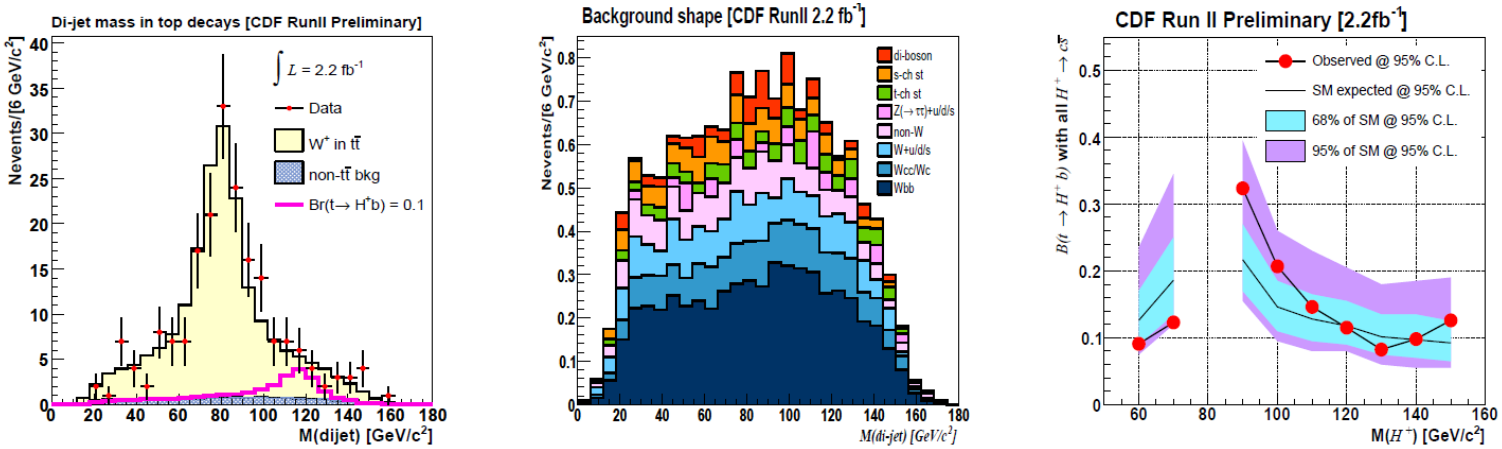

Figure 35. CDF. Left: di-jet mass in top decays. Center: background contributions to the di-jet mass in top decays. Right: model-independent BR(t → H^+b) limit for BR(H^+ → c$\bar{s}$) = 1. In order to cover any generic anomalous charged Higgs boson, the search is extended below the W mass.

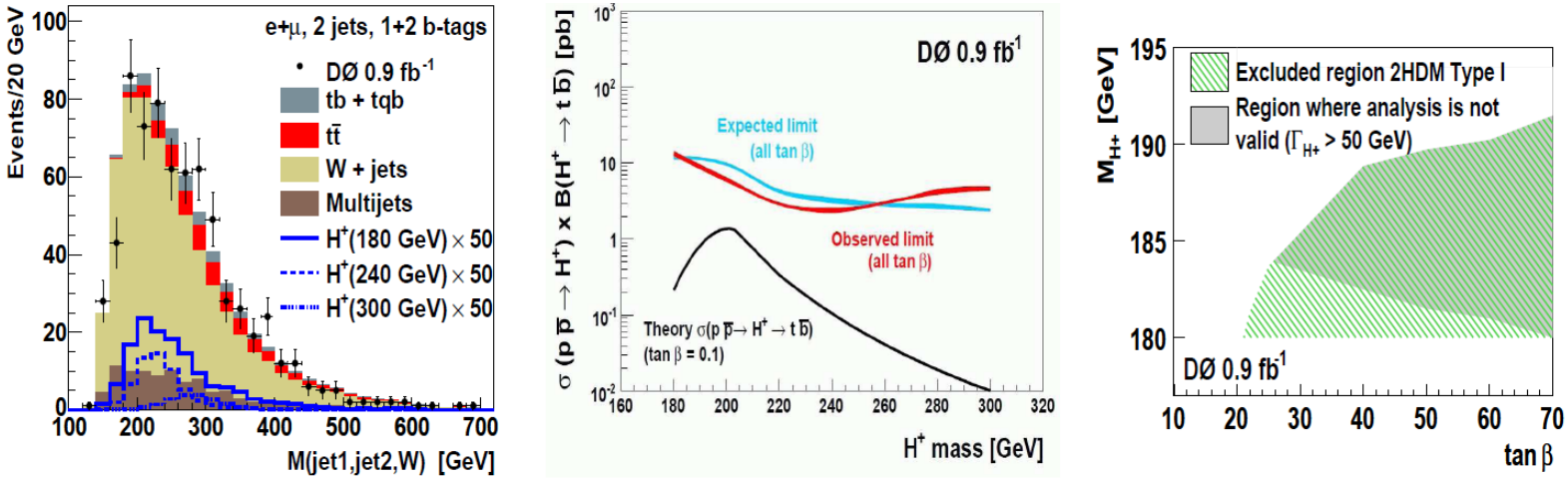

Figure 36. DØ. $p\bar{p} \to H^+ \to t\bar{b}$. Left: invariant charged Higgs boson mass (type III model). Center: cross-section limit in THDM (type II). Right: THDM excluded regions for model type I.

Beyond the SM: H→γγ

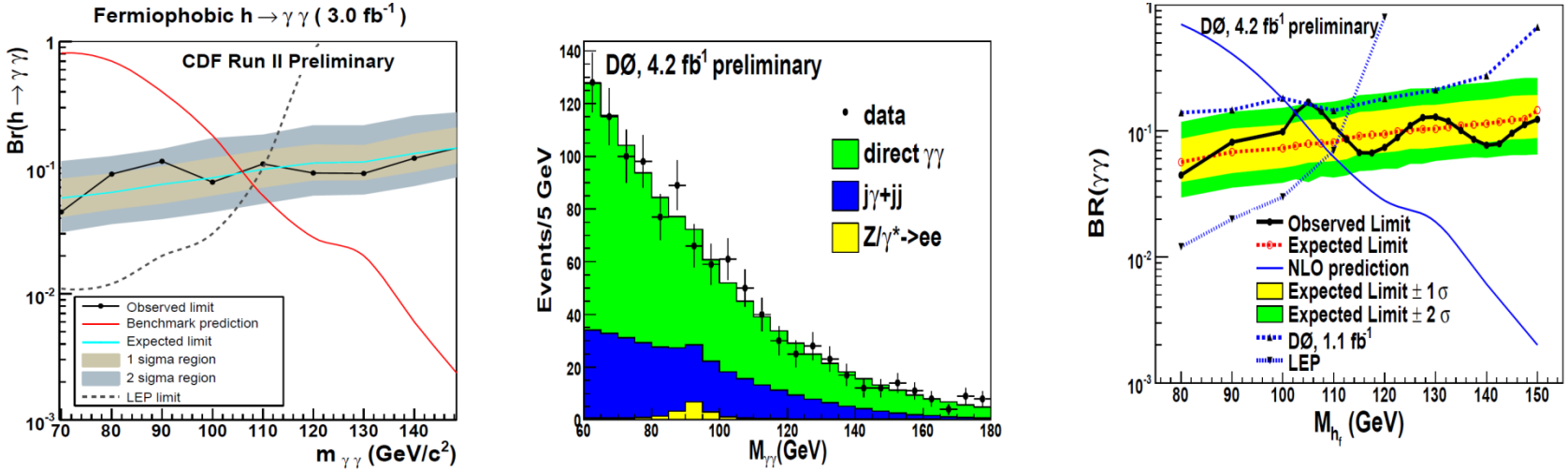

Figure 37. Fermiophobic Higgs. H → γγ. Left: CDF limits at 95% CL with $\mathcal{L} = 3.0$ fb^{-1}. Center: DØ invariant γγ mass distribution with $\mathcal{L} = 4.2$ fb^{-1}. Right: DØ limits at 95% CL with $\mathcal{L} = 4.2$ fb^{-1}.

Beyond the SM: H^{++}

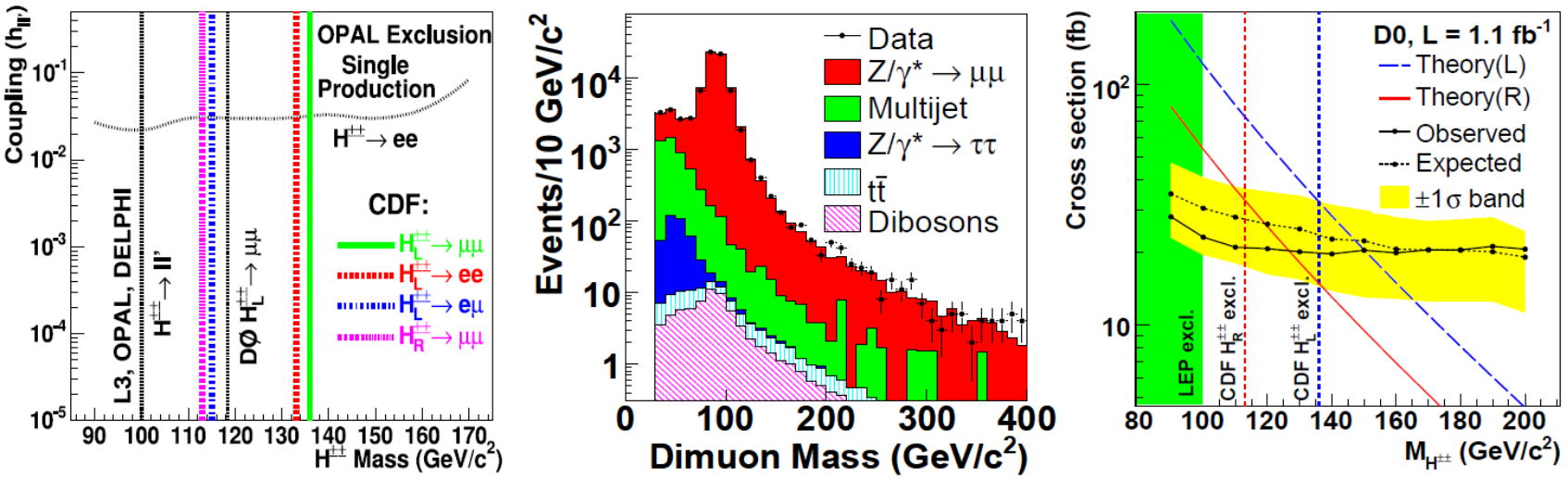

Figure 38. Left: CDF doubly-charged Higgs boson mass limits at 95% CL. Center: DØ di-muon mass spectrum. Right: DØ doubly-charged Higgs boson mass limits at 95% CL.

Conclusions

- Run-II Tevatron limits exceed some LEP limits.
- SM Higgs: Gluon fusion with WW decays, associated production WH with bb and WW decays and ZH→ ννbb. More recently ZH→llbb, H→$\gamma\gamma$ and tt→ttH.
- Beyond the SM: bbA, H^+, H^{++}, h→$\gamma\gamma$,$\tau\tau$.
- Collaboration of phenomenologists and experimentalists crucial to fully exploit potential of collected data.
- Sensitivity increase significantly faster than from increased statistics alone. By end of 2010 the full SM mass range will be covered up to about 180 GeV by 2 to 3 sigma.

References

[1] A. Sopczak, Proceedings QFTHEP'04, St. Petersburg, Russia; and WONP'05, Havana, Cuba, hep-ph/0502002, and references therein.

[2] A. Sopczak, "MSSM Higgs boson searches at LEP", Talk at the 13th International Conference on Supersymmetry and Unification of Fundamental Interactions (SUSY'05), Durham, UK, July 18-23, 2005, hep-ph/0602136.

[3] The LEP Electroweak Working Group, http://lepewwg.web.cern.ch/LEPEWWG/.

[4] A. Sopczak, hep-ph/0605236. FERMILAB-CONF-06-134-E-T, May 2006. Presented at Aspen Summer Workshop on Collider Physics: from the Tevatron to the LHC to the Linear Collider, Aspen, Colorado, 15 August - 11 September, 2005.

[5] CDF and DØ Collaborations, summary of SM cross-section measurements.

[6] T. Aaltonen et al., CDF Collaboration, Phys. Rev. Lett. **100**, 201801 (2008).

[7] V. M. Abazov et al., DØ Collaboration, Phys. Rev. Lett. **101**, 171803 (2008).

[8] Fermilab Operations, http://www-bdnew.fnal.gov/operations/lum/lum.html.

[9] F. Maltoni et al. in TeV4LHC Workshop, Fermilab, Chicago, October 2005. hep-ph/0612172.

[10] A. Djouadi, J. Kalinowski and M. Spira, Comput. Phys. Commun. **108**, 56 (1998).

[11] C. S. Hill, CDF Collaboration, Nucl. Instrum. Meth. **A 530**, 1 (2004).

[12] DØ Collaboration, R. Lipton, private communications (2009).

[13] I. Iashvili in TeV4LHC Workshop, Fermilab, Chicago, October 2005. hep-ph/0612172, and updated plot.

[14] A. Haas, "A Search for Neutral Higgs Bosons at High $\tan\beta$ in Multi-jet Events from $p\bar{p}$ Collisions at $\sqrt(s) = 1960$ GeV", University of Washington, PhD Thesis (2005).

[15] J. Donini et al., Nucl. Instrum. Meth. **A 596**, 354 (2008).

[16] T. Altonen et al., CDF Collaboration, arXiv:0812.4458, submitted to Phys. Rev. D.

[17] V. M. Abazov et al., DØ Collaboration, Phys. Rev. Lett. **94**, 161801 (2005).

[18] DØ Collaboration, DØ note 5871, March 6, 2009.

[19] CDF Collaboration, CDF note 9500, July 25, 2008, and update Moriond'09.

[20] CDF Collaboration, CDF note 9463 (ME+BDT analysis), August 8, 2008; CDF note 9468 (NN analysis), August 1, 2008; and CDF note 9596 (combined ME+BDT and NN limit), November 19, 2008.

[21] DØ Collaboration, DØ note 5828, February 5, 2009.

[22] CDF Collaboration, CDF note 7307, December 19, 2008.

References

[23] DØ Collaboration, DØ note 5873, March 13, 2009.
[24] CDF Collaboration, CDF note 9665, December 11, 2008.
[25] DØ Collaboration, DØ note 5876, March 12, 2009.
[26] CDF Collaboration, CDF note 9642, July 11, 2008 and public web page December 29, 2008.
[27] DØ Collaboration, DØ note 5586, February 29, 2008.
[28] CDF Collaboration, CDF note 9248, February 22, 2008.
[29] DØ Collaboration, DØ note 5883, March 9, 2009.
[30] CDF Collaboration, CDF note 9586, October 29, 2008.
[31] DØ Collaboration, DØ note 5858, February 24, 2009.
[32] S. Lai, "Search for Standard Model Higgs Boson Produced in Association with a Top-Antitop Quark Pair in 1.96 TeV Proton-Antiproton Collisions", University of Toronto, PhD Thesis (2006), CDF note 9508; A. Anastassov et al. CDF and D0 Collaborations, AIP Conf. Proc. **903**, 73 (2007).
[33] DØ Collaboration, DØ note 5739, July 28, 2008.
[34] CDF and DØ Collaborations, CDF note 9713, DØ note 5889, March 12, 2009.
[35] CDF and DØ Collaborations, "Projections", http://www-cdf.fnal.gov/physics/new/hdg/results/.
[36] J. Campbell, R. K. Ellis, F. Maltoni and S. Willenbrock, Phys. Rev. **D 67**, 095002 (2003).
[37] S. Dawson, C. B. Jackson, L. Reina and D. Wackeroth, Phys. Rev. **D 69**, 074027 (2004); S. Dittmaier, M. Krämer and M. Spira, Phys. Rev. **D 70**, 074010 (2004).
[38] V. M. Abazov et al., DØ Collaboration, Phys. Rev. Lett. **95**, 151801 (2005).
[39] CDF Collaboration, CDF note 9284, April 7, 2008.
[40] DØ Collaboration, DØ note 5726, July 25, 2008.
[41] CDF Collaboration, CDF note 9071, October 22, 2007.
[42] DØ Collaboration, DØ note 5728, July 25, 2008, and note 5740, July 29, 2008.
[43] DØ Collaboration, DØ note 5715, July 25, 2008.
[44] A. Abulencia et al., The CDF Collaboration, Phys. Rev. Lett. **96**, 042003 (2006).
[45] V. Abazov, DØ Collaboration, Phys. Rev. Lett. **100**, 192003 (2008); DØ note 5371, March 13, 2007; DØ note 5466, August 14, 2008.
[46] CDF Collaboration, CDF note 9322, August 1, 2008.
[47] DØ Collaboration, submitted Phys. Rev. Lett. (2008). arXiv:0807.0859; and cross-section limit released to Summer Conferences 2008.
[48] DØ Collaboration, DØ note 5880, March 11, 2009.
[49] D. Acosta et al., CDF Collaboration, Phys. Rev. Lett. **95**, 071801 (2005).
[50] V.M. Abazov et al., DØ Collaboration, Phys. Rev. Lett. **101**, 071803 (2008).